Journal of Intelligent & Robotic Systems (2018) 91:85–99
https://doi.org/10.1007/s10846-018-0852-2

Bio-Inspired Robotics: A Spatial Cognition Model integrating Place Cells, Grid Cells and Head Direction Cells

Gonzalo Tejera[1] · Martin Llofriu[2] · Alejandra Barrera[3] · Alfredo Weitzenfeld[2]

Received: 3 April 2018 / Accepted: 17 April 2018 / Published online: 4 June 2018

Abstract

The paper presents a bio-inspired robotics model for spatial cognition derived from neurophysiological and experimental studies in rats. The model integrates Hippocampus place cells providing long-term spatial localization with Enthorinal Cortex grid cells providing short-term spatial localization in the form of "neural odometry". Head direction cells provide for orientation in the rat brain. The spatial cognition model is evaluated in simulation and experimentation showing a reduced number of localization errors during robot navigation when contrasted to previous versions of our model.

Keywords Spatial cognition · Robot navigation · Place cells · Grid cells · Head direction cells

1 Introduction

Spatial cognition relates to cognitive processes in the brain required to support spatial localization and navigation in animals and humans. It is believed that the brain builds an internal cognitive map made up primarily of place, grid and head direction cells, as shown in Fig. 1. Historically, Tolman [66] proposed the idea of rats having an internal cognitive map. These studies were followed by O'Keefe [49–52] who identified place cells in the Hippocampus as the location of such a cognitive map. Later studies proposed the notion that the cognitive map integrated external information from the environment and internal information to the rat as part of a path integration system [19, 21, 33, 40, 44, 54]. More recently, Moser and Moser [22, 29, 47] identified the existence of grid cells located in the Entorhinal Cortex (EC) as part of a "neural odometry" system for rat navigation. Ranck [56] discovered the existence of head direction cells in the brain. Together, place, grid and head direction cells are believed to provide for the underlying neural mechanisms required by the brain to build the cognitive map.

While we have a more extensive understanding of the cognitive map functionality in the mammalian brain and its role in spatial navigation there are still many open questions. For example, it is not clearly understood how: (a) grid cells integrate with place cells, and (b) how this integration may provide for more stable long–term localization. The models developed by our group, and others, are intended to address these two issues, among others. While the original model developed by Barrera and Weitzenfeld [5–7] explored the integration of place cell with a path integration module to reproduce goal-oriented learning tasks in rats, this model generated many localization errors during long-term robot navigation. The model developed by Tejera et al. [64, 65] proposed replacing the path integration module found in the Barrera and Weitzenfeld model with a grid cell module that also included head direction cells module as part of the cognitive map. To address the high number of localization during robot navigation, Tejera et al. introduced the concept of a "reset" mechanism to stabilize grid cell firing affecting

✉ Alfredo Weitzenfeld
aweitzenfeld@usf.edu

Gonzalo Tejera
gtejera@fing.edu.uy

Martin Llofriu
mllofriualon@mail.usf.edu

Alejandra Barrera
abarrera@itam.mx

[1] Facultad de Ingeniería, Universidad de la República, Montevideo, Uruguay

[2] Computer Science and Engineering, University of South Florida, Tampa, FL, USA

[3] Departamento de Computación, Instituto Tecnológico Autónomo de Mexico, Mexico City, Mexico

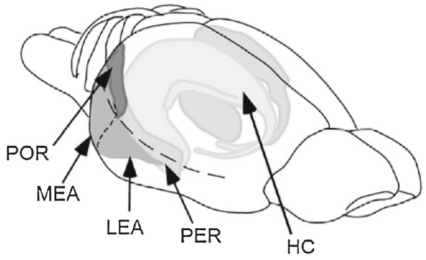

Fig. 1 Hippocampus (HC), Entorhinal Cortices (LEA – Lateral Entorhinal Area, and MEA – Medial Entorhinal Area), Perirhinal Cortex (PER), and Postrhinal Cortex (POR) [1]. (Reproduced with permission from [1])

place cell firing in order to reduce the number of localization errors. The model described in the current paper describes both the proposed integration of grid cells and place cells as part of a cognitive map architecture for robot navigation while contrasting the number of localization errors between the different models by Barrera and Weitzenfeld, and Tejera et al. In particular, the current paper extends upon the results described in [65].

The paper is organized as follows: Section 2 summarizes the main neural components involved in spatial cognition in rats as basis for our model; Section 3 describes our spatial cognition modeling; Section 4 describes spatial localization based on the model; Section 5 describes robot navigation based on the spatial cognition model; Section 6 describes experiments and results; and Section 7 provides conclusions and discussion.

2 Spatial Cognition in Rats

Spatial cognitions neurophysiological studies in rats have shown to integrate place, grid and head direction cells. These studies were made in conjunction with experimental tasks involving classic environment configurations, such as the "T-maze" and "8-arm radial maze" used by O'Keefe [50–52], and the "open maze" used by Morris [45, 46]. In Fig. 2 a sample rat trajectory is shown (top row) based on recordings from Hafting et al. [29] on an open maze environment. Figure 2 shows the corresponding place cell firing at a unique location (mid row), and corresponding grid cell firing at multiple locations resulting in an hexagonal configuration (bottom row). These cells are further discussed in the following sections.

2.1 Place Cells

Place cells are pyramidal neurons in the hippocampus that fire at a specific location in space. O'Keefe [51] discovered place cells from individual recordings of pyramidal cells found in hippocampal substructures CA1 and CA3. These neurons were called place cells because of the high correlation between their firing and the rat location in the environment, thus suggesting their role as a neural substrate for internal spatial representations in the brain. Place cell activity appeared to be dependent on the location of external landmarks or visual cues in the environment [39, 48]. It has been shown that place cells maintain their fields even in the dark [33], and even when some of the visual cues are removed from the environment [55]. Furthermore, it is believed that the response of place cells is derived from combining kinesthetic and visual cues information [28]. Existing studies show that CA3 is able to execute non-linear transformations of sensory input patterns, while CA1 represents input changes in a linear fashion [36], suggesting that representations in CA1 and CA3 emerge independently [37].

2.2 Grid Cells

Grids cells are neurons that fire at multiple locations tessellating an entire surface with a periodic triangular pattern, each described by a number of parameters: spacing, orientation, and phase. Moser and Moser [28, 29] identified grid cells from recordings in the entorhinal cortex. Grid cells appear to be part of a universal spatial metric system, i.e., a "neural odometry" for rat navigation. Further studies showed that in a sufficiently large experimental environment, many entorhinal cortex cells exhibit a grid-like structure firing at regular intervals over the entire environment that is not seen anywhere in the hippocampus [38]. This grid has a hexagonal shape with internal 60° and 120° angles. The spatial coordinate system defined by the grid cell network appears to become anchored to specific landmarks of an individual environment. Additionally, grids assume similar phases and orientations with respect to external landmarks on repeated exposures to the same environment, irrespective of where the animal starts its navigation [29, 41, 48]. The geometrical structure and spacing of grid fields seems independent of the size and shape of the environment. Additionally, grid spacing and grid orientation of neighboring grid cells is almost identical but their grids are offset relative to each other with all grid offsets (phases) equally represented within a small region of the entorhinal cortex. Grid cells fire in response to a particular location, direction and speed. The same group of grid cells responds when the rat is oriented towards different directions remaining in the same physical location [47].

2.3 Head Direction Cells

Head direction cells are found in many cortical regions including the entorhinal cortex [56, 62, 63]. These cells encode the rat's allocentric heading in the azimuthal plane.

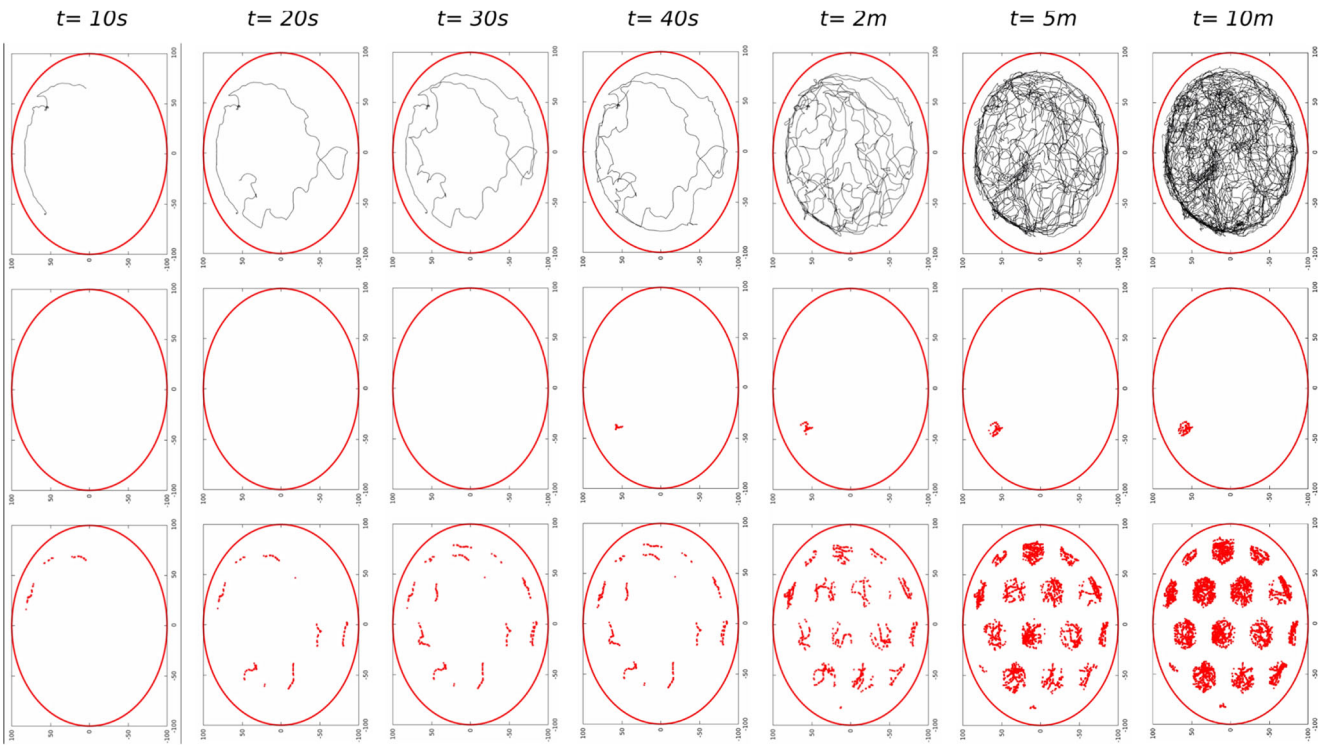

Fig. 2 (Top row) Rat trajectory recorded by Hafting et al. [29]. (Mid row) Single place cell recorded in a unique field location. (Bottom row) Firing of a single MEC grid cell at multiple locations

A head direction cell fires maximally only when the rat's head is oriented towards a specific direction with respect to the environment, regardless of the head orientation relative to the body, the rat's location, or its ongoing behavior. In this way, head direction cells can be seen as an internal compass. Just like place cells and grid cells, the activity of head direction cells is driven both by visual cues and egocentric motion signals, enabling the rat to maintain and update the activity in its head direction cells even when moving around in darkness [16, 58].

3 Spatial Cognition Modeling

Various spatial cognition models have been developed in the past. Most of these models are based exclusively on place cells models, while some provide some level of integration with grid cells and head direction cells. These models are further discussed in [6, 7] corresponding to [2–7, 10, 12, 15, 18, 20, 23, 27, 42, 43, 57, 59, 64, 65]. These models evaluate different aspects of spatial cognition including in some cases using both simulation and robotics experimentation. The rest of this section describes our group's spatial cognition model, which is summarized in Fig. 3.

An important aspect of our group's spatial cognition model is that it relates spatial cognition processes including learning and memory by (i) interaction of different brain structures to demonstrate skills associated with global and local localization in space, (ii) path integration, (iii) use of kinesthetic and visual cues during orientation, (iv) generation of topological-metric spatial representation, (iv) adaptation using Hebbian learning [31], (v) representation of internal motivational states based on hunger and thirst drives, and (vi) management of rewards by use of reinforcement learning using an Actor-Critic architecture [4, 8, 32]. The learning architecture is complemented by applying backward reinforcement to successful routes followed by the rat during training thus enabling learning of explored routes. After exploration, the model exploits maximum reward expectations to guide the rat towards the goal from any given departure location. Additionally, the model implements an on-line learning process to adapt the cognitive map to changes in the physical configuration of the environment.

The different components of the model, shown in Fig. 3, include:

- Motivation module, related to the rat's lateral hypothalamus [34]. It computes the immediate reward the rat gets by the presence of goals (r).
- Kinesthetic module, involving the participation of the posterior parietal cortex (PPC) [53] and the retrosplenial cortex (RC) [17]. It represents the updated egocentric position of the rat's point of departure by

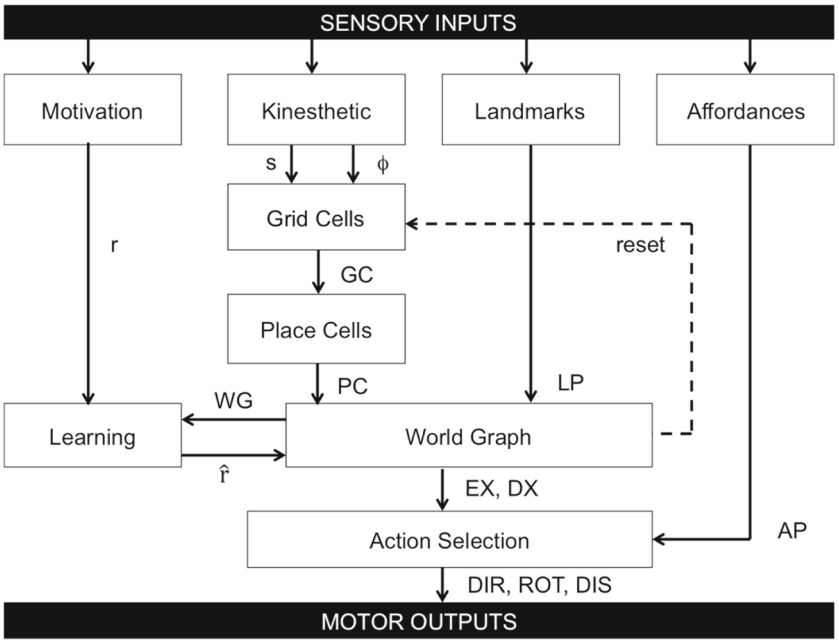

Fig. 3 The diagram describes an extension to the original Barrera and Weitzenfeld [7] spatial cognition model

activating groups of neurons that respond to specific kinesthetic information patterns.

- Landmarks module, encoding global spatial positioning.
- Affordances module, mapped to PPC [39]. It generates the affordances perceptual schema (AP) encoding possible turns the rat can perform at any given time being at a specific location and orientation [24, 25].
- Grid Cells module, corresponding to the rat's entorhinal cortex. It receives kinesthetic information in the form of rat speed (s) and orientation (Φ). Additionally, a reset mechanism provides recalibration feedback from the World Graph to the Grid Cells module to prevent grid cell activity from drifting over time.
- Place Cells module, corresponding to the rat's hippocampus; it receives input from grid cells. Connections between different place cell layers are strengthened by Hebbian learning [31].
- World Graph module, receiving input from Place Cells and Landmarks modules in order to produce topological patterns representing unique locations in the environment. This module associates place fields with a physical location in the environment that is identified by an activity pattern (PC) and whose extension is determined by affordances (AP) sensed by the rat during exploration. The world graph layer integrates kinesthetic and landmark information [33] mapped to the prelimbic cortex [26]. It stores those associations in a spatial representation and performs place recognition. The Actor units store the activation patterns PC associated with the landmark processing patterns LP, one for each direction, and every connection is associated with a weight, representing the expectation of getting the biggest reward (EX) when orienting in a particular direction (DX) towards the goal.
- Learning module, corresponding to dopaminergic neurons in the ventral tegmental area and to ventral striatum processing reward information based on a Actor-Critic reinforcement learning architecture [8, 60].
- Action Selection module, computing the motor outputs of the model: direction (DIR), rotation (ROT) and displacement (DIS). Motion is determined by considering the current AP, the selection of a random rotation between possible affordances, the curiosity to execute rotations not yet explored, and the expectations of maximum reward (EX, DX).

Figure 4 provides the physical setup for running experiments using a *Khepera* robot as it navigates a "dry" circular arena of the open water maze by Morris [45, 46]. The figure shows a "Global Image" illustrating output taken from a "Panoramic Image" obtained from local robot cameras that provide multiple "Local Views" showing a number of fixed color visual cues perceived by the "Landmarks" module. The orientation and distance to the different visual cues are used to build the topological map shown in the "World Graph" layer and used by the "Action Selection" module to produce robot motion actions.

4 Spatial Localization

Spatial localization in our model integrates short term localization produced by grid cells with long term localization produced by place cells, as shown in Fig. 5. The figure

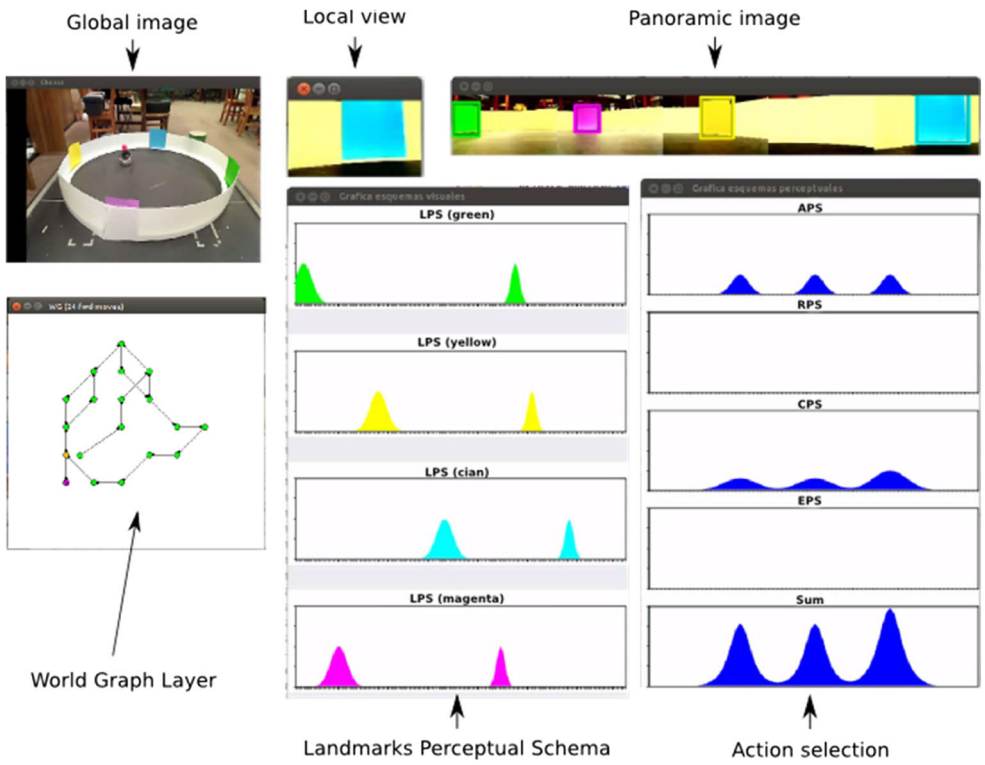

Fig. 4 The "Global Image" in the top left corner shows a robot navigating a "dry" Morris open water maze. The "Local View" in the top middle image shows the view from the robot local camera. The "Panoramic Image" in the top right side is a composition of multiple robot local camera views. The bottom left "World Graph Layer" node diagram in green represents the topological map of locations previously visited by the robot, with current position in magenta and previous one in yellow. The "Landmark Perceptual Schema (LPS)" in the bottom middle figure shows a number of landmarks in different colors where left Gaussians represent orientations as shown in the "Panoramic Image", while the right Gaussians represent distances from the robot for each colored landmark (magenta, cyan, yellow and green). The "Action Selection" diagram in the bottom right represents the three possible motion outputs each having 3 possible activities obtained from the "Expectation of Maximum Reward" (EMR), "Expectation Perceptual Schema" (EPS), "Curiosity Perceptual Schema" (CPS), "Random Perceptual Schema" (RPS), or "Affordance Perceptual Schema" (APS). The highest value of the 3 sum values correspond to moving left, right, or forwards, in a winner-take-all fashion

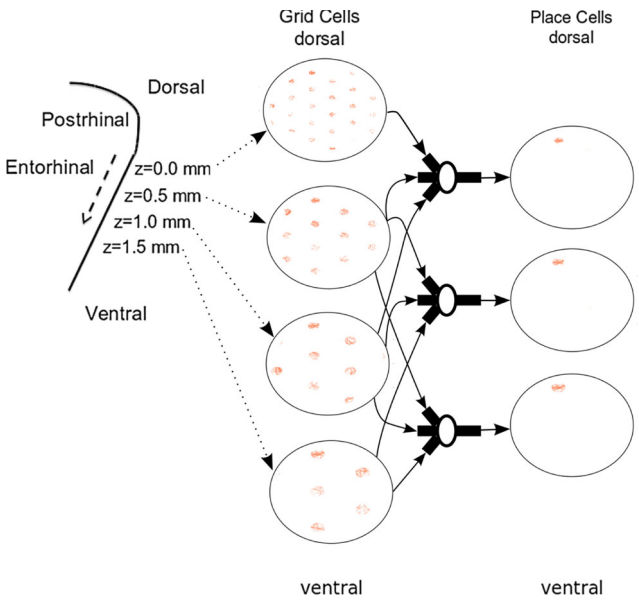

Fig. 5 The illustration shows the proposed grid cell to place cell interconnectivity [29, 61]

illustrates grid cell patterns with increased spaces between firing along the z-axis in MEC [29, 61]. The grid cells combine to generate unique place cell firing locations in the hippocampus.

4.1 Short-Term Localization

We use a linear interference oscillator to generate grid cells firing patterns [30]. The numerical values for z were obtained heuristically according to Table 1, where T(z) is the oscillation period, f(z) corresponds to the oscillation frequency (inverse of T(z)), and G(z) represents the grid cell spacing function [13].

Equations 1, 2 and 3 describe the different oscillatory values based on the distance z from the postrhinal border [30].

$$T(z) = 0.094z + 0.13 \quad (1)$$

$$f(z) = 1/T(z) \quad (2)$$

$$f(z) = 1/(0.094z + 0.13) \quad (3)$$

Table 1 Grid Cell Firing Spacing

z(mm)	Grid cell firing		
	$T(z)$ (sec)	$f(z)$ (Hz)	G(z) (cm)
0.00	0.1300	7.6923	39.00
0.25	0.1535	6.5147	46.05
0.50	0.1770	5.6497	53.10
0.75	0.2005	4.9875	60.15
1.00	0.2240	4.4643	67.20
1.25	0.2475	4.0404	74.25
1.50	0.2710	3.6900	81.30

Equation 4 describes the grid cell field spacing $G(z)$ (cm) depending on the dorsal–ventral position z (mm). The grid cell spacing function $G(z)$ and the oscillation period function $T(z) = 1/f(z)$ can be scaled to each other by a constant H =300 defined to estimate the spacing $G(z)$ given an oscillation frequency f of approximately 300 Hz per cm.

$$G(z) = H/f(z) \tag{4}$$

The linear oscillatory interference model [30] is summarized in the following equations where the membrane voltage oscillation $V(t)$ is given by (5) by applying a cosine function "cos" to the soma and dendritic oscillations at frequencies f_s and f_d, respectively.

$$V(t) = \cos(f_s 2\pi t) + \cos(f_d 2\pi t) \tag{5}$$

As described in Eq. 6, f_b (the "beat" frequency) is obtained from the difference of f_s and f_d, i.e. $f_b = f_d - f_s$, or $f_d = f_s + f_b$, as illustrated in Fig. 6.

$$f_d = f_s + f_b \tag{6}$$

As described in Eq. 7, the rat velocity v is determined from its speed s and the difference between head direction ϕ and the preferred head direction ϕ_{HD}.

$$v = s\cos(\phi - \phi_{\mathrm{HD}}) \tag{7}$$

As described in Eq. 8, the distance between two firing locations can be determined from spatial wavelength λ_{b}, by multiplying velocity v with the beat period T_{b}.

$$\lambda_b = vT_b = v/f_b = s\cos(\phi - \phi_{\mathrm{HD}})/f_b \tag{8}$$

As described in Eq. 9, $\lambda_b$can remain constant by defining a beat frequency f_b,

$$f_b = Bs\cos(\phi - \phi_{\mathrm{HD}}) \tag{9}$$

where the threshold activation constant $B = 1/\lambda_b$ corresponds to the inverse of the spatial wavelength λ_b. The dendrite oscillation frequency f_{d} can then be redefined as in Eq. 10,

$$f_d = f_s + Bs\cos(\phi - \phi_{\mathrm{HD}}) \tag{10}$$

where $B = 0.00385$, that can be redefined in terms of B_{H} and $f(z)$, as shown in Eq. 11.

$$B = B_{\mathrm{H}} f(z) \tag{11}$$

The dendrite frequency f_{d} can be rewritten as described in Eq. 12.

$$f_d = f_s + f_s B_{\mathrm{H}} s\cos(\phi - \phi_{\mathrm{HD}}) \tag{12}$$

As described in Eq. 13, grid cell firing $gc(t)$ can be obtained by combining three band cells, each corresponding to $V(t)$. The linear oscillatory interference model implemented in our spatial cognition model combines band cells varying in

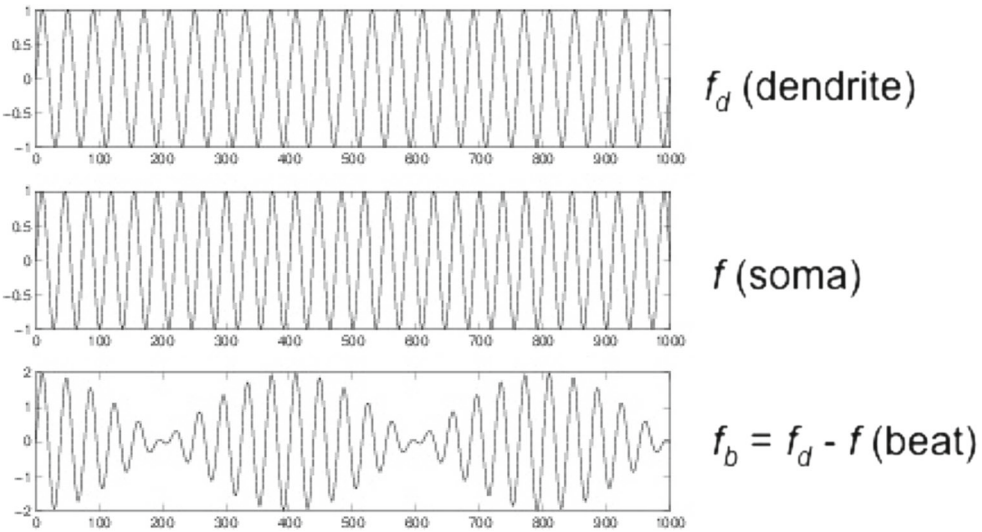

Fig. 6 Example of two oscillations at very close frequencies, f_d and f_s, added together to generate the "beat" oscillation f_b at a lower frequency. (Reproduced with permission from [65])

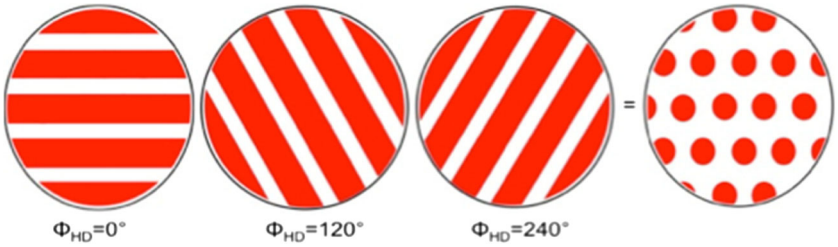

Fig. 7 Generation of a single Grid Cell (right) firing obtained from three Band Cells varying in 120° [12, 29]. The band cells (leftmost three) fire in fixed bands of the environment (red). The grid cell (rightmost) fires in the intersection of the three band cells [65]. (Reproduced with permission from [65])

120° to produce individual grid cell as shown in Fig. 7 [30, 35, 40].

$$gc(t) = \Theta\left[\prod_{HD}(\cos(f_s 2\pi t) + \cos((f_s + f_s B_H scos(\phi - \phi_{HD}))2\pi t) + \varphi\right] \quad (13)$$

4.2 Long-Term Localization

Each place cell activation pc is generated by applying a step function Θ to the sum of N grid cells gc with similar initial phase as given by Eq. 14.

$$pc(t) = \Theta\left(\sum_{i=1}^{N_{gc}} gc_i(t)\right) \quad (14)$$

In Eq. 14, N_{gc} represents the number of grid cells and $gc_{\mathrm{i}}(t)$ corresponds to the function defined in Eq. 13. This equation proposes a weighted sum of grid cell firing to generate place cell firing based on work by Solstad et al. [61]. The values are selected considering their ventro-dorsal position at the time the grid cells and place cells are created, and stay fixed during the experiment. Solstad et al. [61] summed the output of 10 grid cells with different spacing and same phases and orientations after applying a global inhibition during the formation of a unique place cell in the environment. The output of the Place Cell (PC) module consists of all place cells from Eq. 14.

Figure 8 illustrates place cell activation (in the center plot) by combining multiple grid cells with the same spatial phase φ and different spatial orientation ϕ_{HD}. Each of these plots shows activation fields of five different grid cells with spatial orientations ϕ_{HD} varying by increments of 15° from $\phi_{\mathrm{HD}} = -30°$ (yellow) to 15° (purple).

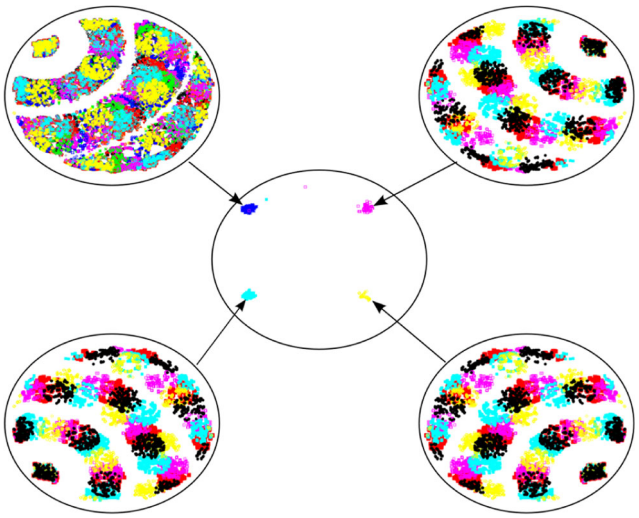

Fig. 8 Each of the four grid cells graphs shows activation fields with spatial orientations ϕ_{HD} varying depending on the initial φ spatial phase incrementing by 15° from $\phi_{\mathrm{HD}} = -30°$ (yellow) to 15° (purple). Each of the four peak grid cell activation fields (at each corner in each of the four graphs) generate the individual place cells firing as shown in the center of the image

5 Robot Navigation

A basic challenge in robotics navigation is for robots to have a good spatial localization in a given environment. Robot navigation in our model is based on the spatial cognition map using a World Graph topology generated from Place Cell activation integrated with the neural odometry from Grid Cells. The following sections describe the world graph and cell firing recalibration intended to reduce localization errors.

5.1 World Graph

The World Graph (WG) generates a topological map of the environment, as shown in Fig. 9 (shown also in Fig. 4). Each node j in WG_j receives input from the Place Cells (PC) and Landmarks (LP) modules multiplied by corresponding weights w_{ij},as described in Eq. 15).

$$WG_j = \sum_i PC_i w_{ij}^{pc} + \sum_i LP_i w_{ij}^{lp} \quad (15)$$

Each World Graph node WG_j in the topological map compares a new pattern $pat \in \mathrm{PAT}$ to all stored WG_i using

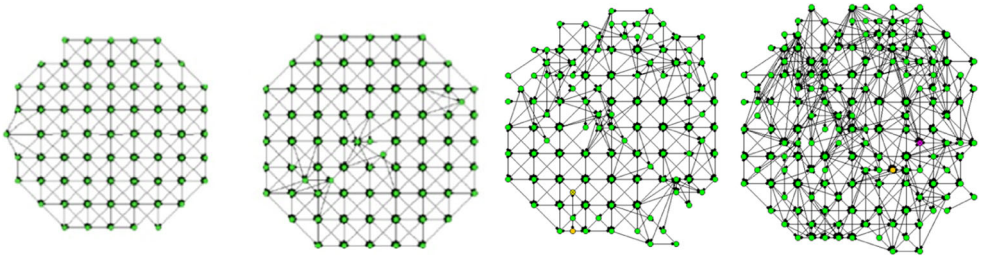

(a) no localization errors (b) 5 localization errors (c) 40 localization errors (d) 100 localization errors

Fig. 9 WG mapping a circular arena: **a** no localization errors, **b** 5 localization errors, **c** 40 localization errors, and **d** 100 localization errors. (Reproduced with permission from [65])

a similarity function (SD) function based on their Euclidean distance, as described in Eq. 16.

$$SD(pat, WG_j) = \sqrt{\sum_{i=1}^{N_{PC}} (pat_i - WG_{ij})^2} \tag{16}$$

If the new pattern *pat* has a low similarity degree (SD) when compared to the existing stored patterns WG_i, then the robot is presumed to be located at an existing WG_j node to update its global localization as described in Eq. 17.

$$pat = arg\ min_{pat \in PAT} SD(pat, WG_j) \tag{17}$$

If no minimum acceptable distance is found between *pat* and WG_j, then a new node is created in WG (see [6] for more details). If too many new nodes are created after the robot has navigated the same environment this would lead to navigation errors where the robot is not recognizing locations where it has already been. Figure 9 illustrates this problem by showing sample WG maps obtained with different number of localization errors after the robot has navigated a circular arena multiple times.

5.2 Cell Firing Recalibration

To overcome localization errors in WG, every time a valid $pat = WG_j$ is found; a recalibration *reset* signal is applied to the corresponding grid cell. Figure 10 shows the reset signal sent from the World Graph back to the Band Cells that connects to the Grid Cells. Additional parameters shown in the figure include linear velocity s, angular velocity ω, and head direction information ϕ.

If we look back at Eq. 5, shown again here in Eq. 18, we can apply the *reset* signal to the dendritic phase of $V(t)$ corresponding to $gc(t)$, as described by Eq. 18.

$$V(t) = \cos(f_s 2\pi t) + \cos(f_d 2\pi t) \tag{18}$$

The soma components from Eq. 18 can be redefined as $x_s(t)$ and $x_d(t)$, respectively as shown in Eqs. 19 and 20.

$$x_s(t) = f_s 2\pi t \tag{19}$$
$$x_d(t) = f_d 2\pi t \tag{20}$$

In Eq. 21, the new dendritic component $x'_d(t)$ enables $x_d(t)$ to get closer to $x_s(t)$.

$$x'_d(t) = x_d(t) + \gamma(x_s(t) - x_d(t)) \tag{21}$$

If γ is set to 0, then no reset update is made to $x'_d(t)$, while setting γ to 1 would make $x'_d(t)$ equal to $x_s(t)$. Equation 22) summarizes the reset mechanism.

$$x'_d(t) = \begin{cases} x_d(t) + y(x_s(t) - x_d(t)) & if SD(winner, WG) < SD_{merge} \\ x_d(t) & otherwise \end{cases} \tag{22}$$

Figure 11 illustrates recalibration using the *reset* mechanism, as follows:

- The first row shows a simple square motion by the rat ending after 4 steps starting from its original location.

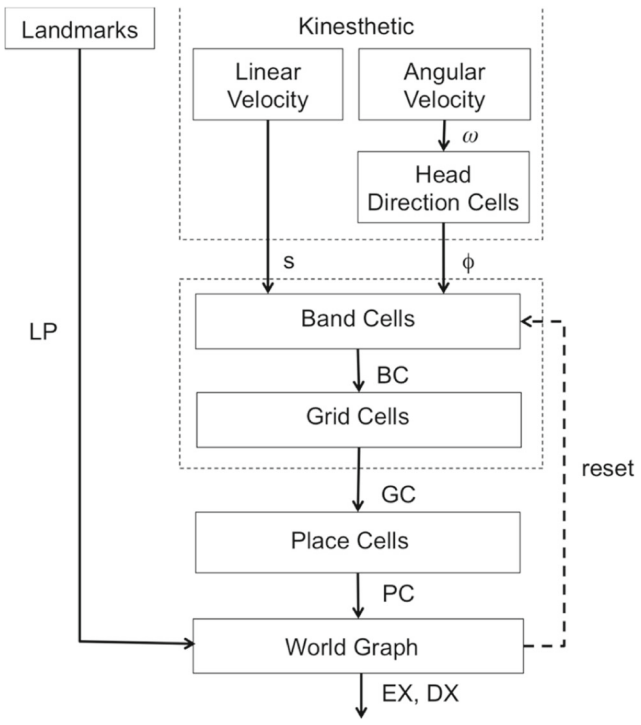

Fig. 10 The diagram describes the components involved in the interference oscillatory model including the reset mechanisms from the World Graph back to the Grid Cells via de Band Cells

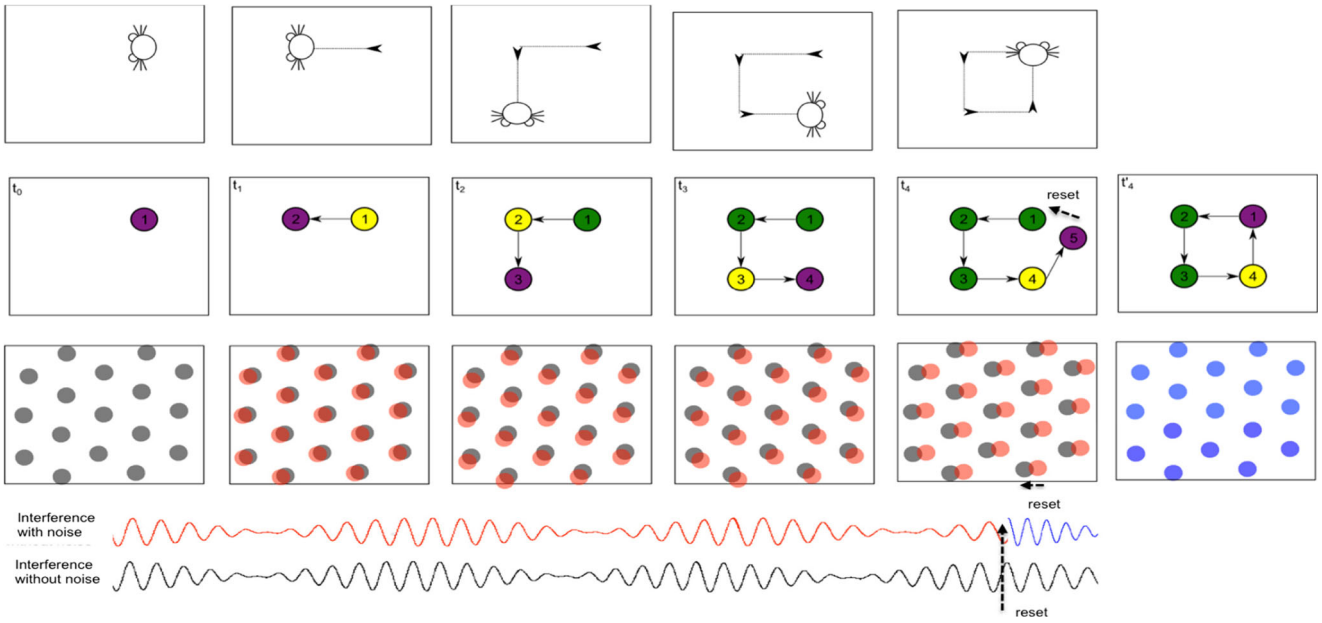

Fig. 11 Illustratation of grid cell recalibration using the reset mechanism. The first row shows a simple square motion by the rat. The second row shows the corresponding WG node localization of the rat matching the square motion. The third row shows two sets of grid cell firing, a dark one corresponding to an ideal noiseless firing and a red one where error is accumulated due to intrinsic or extrinsic noise in the dendritic linear oscillator. The fourth row contrasts the noiseless and noisy grid cell dendritic linear oscillators

- The second row shows the corresponding WG node localization of the rat matching the square motion steps until a new purple node is created at t_4. Considering the closeness of the new purple node to the first node generated at t_0 by the World Graph; a *reset* signal is generated recalibrating node 5 to match node 1. Note that initially a new node is created or a previous one matched depending on the threshold value for SD.
- The third row shows two sets of grid cell firing, a dark one corresponding to an ideal noiseless firing and a red one where error is accumulated due to intrinsic or extrinsic noise in the dendritic linear oscillator. Note that once WG sends the *reset* signal, this will cause a grid cell *reset* signal where the accumulated grid cell activation will modify its phase according to Eq. 22 in trying to get closer to the noiseless dendritic linear oscillator.
- The fourth row contrasts the noiseless and noisy grid cell dendritic linear oscillators. Note that this procedure is performed every time a WG node is compared to existing ones in trying to perform recalibration affecting all grid cells active at the particular location where the WG fires.

6 Experiments and Results

In this section we present experiments and results from grid cell recalibration using the reset mechanism while contrasting the localization errors between our original RatNav1 model, the new RatNav2 model without reset, and the new RatNav2 model with reset. Borenstein and Feng [9] proposed a method for measuring odometry errors in mobile robots by having the robot repeat some motions, while a human operator measured the localization errors between the expected position and actual robot position. This procedure was applied to our experiments to characterize the error and find the μ_{err_num} and $\sigma^2_{err\_num}$ constants. Figure 12 shows the incorporation of noise to robot speed.

To analyze the localization errors, we have added noise to speed s resulting in a noisy speed s', as described by Eq. 23.

$$s' = s(1 + \mathcal{N}(\mu_{err\_num}, \sigma^2_{err\_num}) * factor) \tag{23}$$

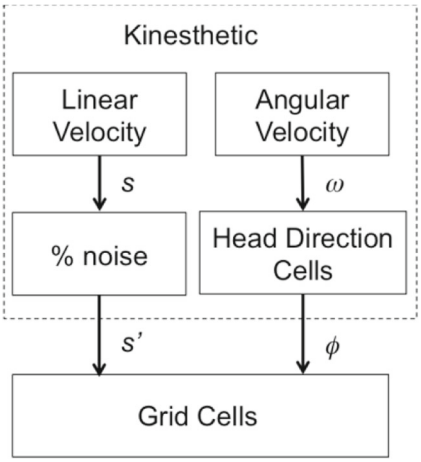

Fig. 12 Incorporation of a noisy speed s'

Table 2 Parameters and corresponding values used during evaluation of the model

Parameter	Description	Value
α_{hebb}	Learning rate applied to different layers in the model	0.001
α_{reset}	Learning rate applied to the dendritic phase in the grid cells when doing reset	0.05
β	Learning rate applied to adapt estimated Q values in the learning module	0.1
γ	Discount factor used by the reinforcement learning module	0.7
θ_g	Grid cell activation threshold	1.8
θ_{sd}	WG similarity threshold for loop closure	110
μ_{err_num}	Mean normal distribution characterizing the robot forward motion error	1.14 mm
$\sigma^2_{err_num}$	Normal distribution standard deviation characterizing the robot forward motion error	0.18 mm
BH	Constant for the grid cell threshold activation	0.00385 s/cm
H	Scale constant for the grid cell threshold activation	300 Hz-cm
N_{FDL}	Number of neurons in the pattern detection layers	400 (20x20)
Ngc	Number of grid cells	880
Ngo	Number of orientations generated by each vertex	10
N_{land}	Number of landmarks	4
nPS	Number of neurons in any linear perceptual schema	80
mm_fwd_move	Millimeters sent to the robot for each forward advance motion	150 mm

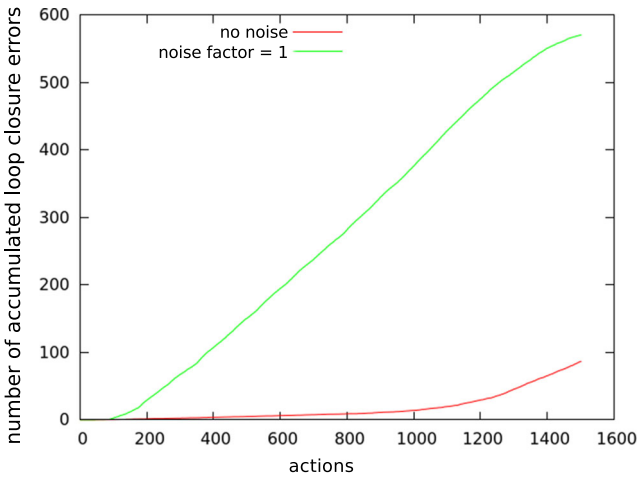

Fig. 13 Localization errors for a simulated robot when running the RatNav1 [6]: red – without noise, green – with noise level factor = 1

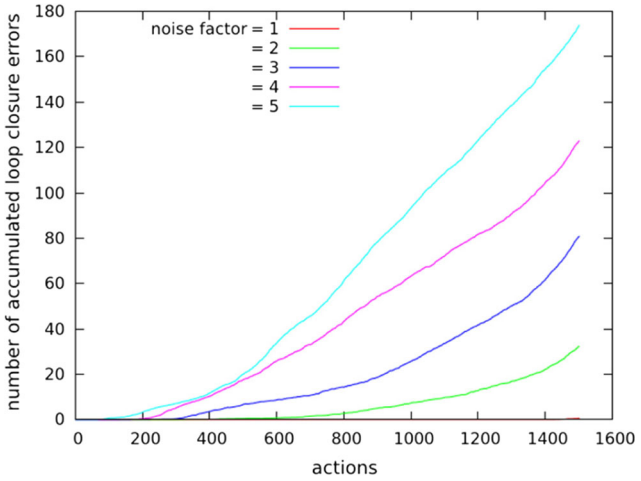

Fig. 14 Localization errors for the RatNav2 model without the reset mechanism

In Eq. 23, $\mathcal{N}(\mu_{err\_num}, \sigma^2_{err\_num})$ represents a random function with normal distribution, and parameters μ_{err_num} and $\sigma^2_{err\_num}$. The *factor* parameter is set between 0 and 5.

Table 2 summarizes the parameters used during evaluation.

6.1 Localization errors for the RatNav1 model

Figure 13 shows the number of localization errors for a simulated robot when running the original RatNav1 [6] without noise (red) and with noise level factor = 1 (green). The results show very limited tolerance to noise, where for noise level = 1, over 500 accumulated localization errors were obtained for about 1,200 motion steps or 20 navigation sessions in the circular open maze.

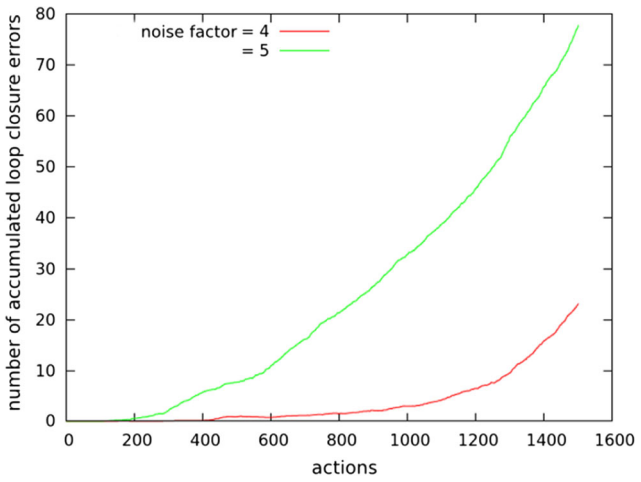

Fig. 15 Localization errors for the RatNav2 model with the reset mechanism

Table 3 Error Comparison during loop closure

Model	$RN1/DRL1$	$RN2/G1$	$RN2/G4$	$RN2/G5$	$RN2/GR4$	$RN2/GR5$
Min	503	0	24	57	0	30
Max	621	4	187	373	51	105
Mean	570	0.57	123	174	23	75
Variance	26	1.33	33	66	15	21

6.2 Localization Errors for the RatNav2 model without Reset

Figure 14 presents the localization errors for our RatNav2 model without the reset mechanism. The results show a better tolerance to noise than the original RatNav1 model. As opposed to the original RatNav1 model, there are very few localization errors when the noise factor = 1 corresponding to the red line over the x-axis. As noise increases errors also increase but without reaching the level found in the RatNav1 model. A total of 30 sessions were performed each resulting in 1,500 motor actions according to Eq. 23.

6.3 Localization Errors for the RatNav2 model with Reset

Figure 15 shows the localization errors for the RatNav2 model with the reset mechanism. The reset mechanism greatly diminishes the number of localization errors. Note that there are no errors for noise factors less than 4.

6.4 Localization Error Contrast between RatNav1 and RatNav2 models

Table 3 provides a comparison of loop closure errors in WG between RatNav1 (RN1/DRLN) and RatNav2 (RN2/GN & RN2/GRN) models for different noise factors $N = 1$ to 5. GN corresponds to the grid cell model without reset, while GRN corresponds to the grid cell model with reset.

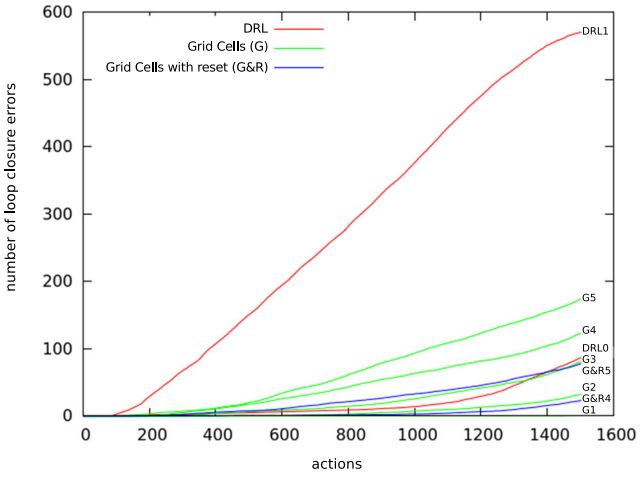

Fig. 16 Localization error comparison based on data from Table 3 [64]. (Reproduced with permission from [65])

Figure 16 presents error values in relation to motion actions based on Table 3. RatNav1/DRL1 had the highest number of errors, while the RatNav2/GN and RatNav2/GRN models (with N varying from 1 to 5) with and without the reset mechanism, respectively, generated the lowest number of errors.

6.5 Multi-Scale Spacing Localization Errors in the RatNav2 Model without and with Reset

The previous results use the minimum observed spacing in MEC grid cells. In this section we present results for different spacing factors z while keeping the rest of the parameters fixed. Different spacing is grouped in the ventral-dorsal axis of MEC in 6 to 10 groups with spacing incrementing geometrically according to (8):

$$G_f(factor_{spc}) = G(0)p^{factor_{spc}-1} \tag{24}$$

Towse et al. [67] analyzed the effect of various spacing values for each grouping in relation to localization with best results obtained with a geometric increase in spacing for p =1.4. Table 4 shows spacing values for the first 3 groups.

Figure 17 (left) presents the number of localization errors for a fixed spacing factor of 1 with noise factor of 2 (noise factor of 0 and 1 showed no errors, while noise factor of 1 showed errors only without the reset mechanism). The results show the increasing number of localization errors without the reset mechanism. Figures 17 (right) shows results for spacing factor of 2 for a noise factor of 2.

Figure 18 (left) shows results for spacing factor of 3 for a noise factor of 2. Figure 18 (right) contrasts localization errors for spacing factors 1, 2 and 3, for a noise factor of 3 without the reset mechanism.

Table 4 Spacing Factor

$factor_{spc}$	Spacing (G − cm)
1	39
2	49
3	69

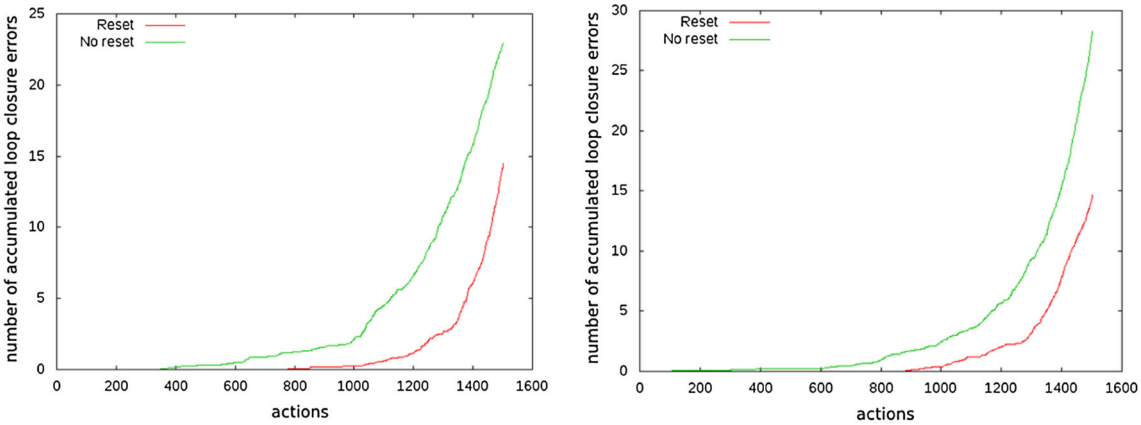

Fig. 17 (Left) Localization errors with spacing factor of 1 and noise factor of 2, reset versus no reset mechanism. (Right) Localization errors with spacing factor of 2 and noise factor of 2, showing reset versus no reset mechanism

Figure 19 contrasts localization errors for spacing factors 1, 2 and 3, for a noise factor of 3 with reset.

7 Conclusions and Discussion

The paper presented a biologically inspired robotics model for spatial cognition that integrates place cells in the Hippocampus, grid cells in the Entorhinal Cortex (EC), and head direction cell, based on work by Tejera et al. [64, 65]. The current paper extends the results from our previous work by contrasting various versions of the model in relation to their stability during long-term robot navigation. When compared to the original RatNav1 model by Barrera and Weitzenfeld [5–7], the RatNav2 model by Tejera et al. [64, 65], reduces the number of localization errors by the introduction of a "reset" mechanism to stabilize both grid cell and place cell firing. The effect of the reset mechanism was analyzed by comparing the effect of different noise factors during simulated robot navigation to mimic different levels of noise found in physical robots. A particular difference between the two different versions of our model has been the use of a grid cell module replacing the original path integration module. This new grid cell module is based on a linear interference oscillator model [13, 30]. Another alternative for modeling grid cells that has been explored in the past by other groups has been the use of attractors [11, 14]. An aspect that has facilitated the development of the different versions of our spatial cognition models, and their comparison, is the fact that they were both developed using the Neural Simulation Language [68], supporting also model simulation and physical robot experimentation.

In addition to providing further understanding of the structure and functionality of the brain, a major goal of our models is to inspire new algorithms for robotics. In relation to spatial cognition, our goal is intended to support longer-term robot navigation. As part of this effort we plan to further reduce the number of localization errors by exploring multi-scale organization of grid cells and place cells, suggesting that the brain cognitive map may involve

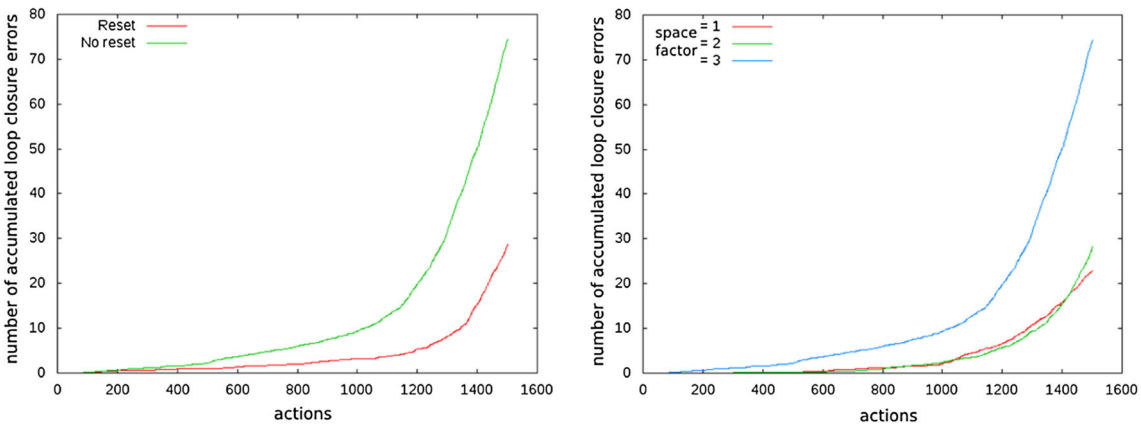

Fig. 18 (Left) Localization errors with spacing factor of 3 and noise factor of 2, reset versus no reset mechanism. (Right) Localization errors for spacing factors 1, 2 and 3 and noise factor of 3 without the reset mechanism

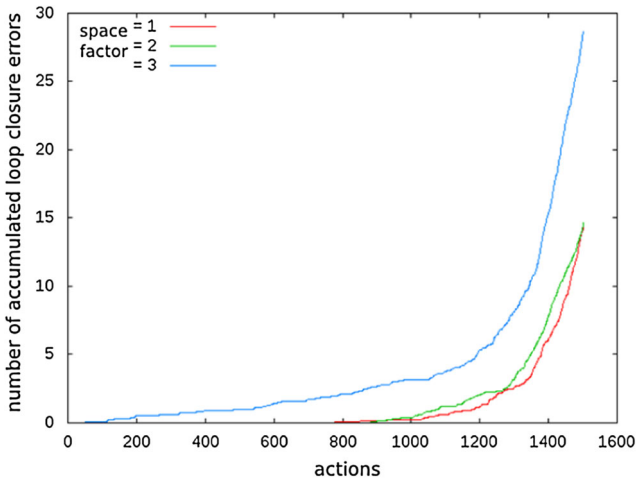

Fig. 19 Localization errors with spacing factor 1, 2 and 3, and noise factor of 3, with the reset mechanism

different field sizes of grid and place cells depending on the complexity of the environment. This would not only reduce the number of grid and place cells involved in an environment but would also provide for remapping or reuse of these cells in multiple environments, an aspect that also relates to limitation in memory and processing in both biological and robotic systems. Finally, as part of future work and as new studies and data are made available by neuroscientists, we expect to extend our spatial cognition models and corresponding experiments with robotic systems.

Acknowledgments This work was funded in part by NSF IIS Robust Intelligence research collaboration grant #1117303 at USF and U. Arizona entitled "Investigations of the Role of Dorsal versus Ventral Place and Grid Cells during Multi-Scale Spatial Navigation in Rats and Robots," and also supported in part by the "Agencia Nacional de Investigacion e Innovación (ANII)" and by the "Asociación Mexicana de Cultura, A. C."

References

1. Agster, K.L., Burwell, R.D.: Hippocampal and subicular efferents and afferents of the perirhinal, postrhinal, and entorhinal cortices of the rat. Behav. Brain Res. **254**, 50–64 (2013). https://doi.org/10.1016/j.bbr.2013.07.005. ISSN 0166–4328
2. Alvernhe, A., Sargolini, F., Poucet, B.: Rats build and update topological representations through exploration. Anim. Cogn. **15**, 359–368 (2011)
3. Antonelo, E., Schrauwen, B.: Unsupervised learning in reservoir computing: modeling hippocampal place cells for small mobile robots. In: Alippi, C., Polycarpou, M., Panayiotou, C., Ellinas, G. (eds.) Artificial Neural Networks - ICANN 2009, volume 5768 of Lecture Notes in Computer Science, chapter 77, pp. 747–756. Springer, Berlin (2009). ISBN 978-3-642-04273-7
4. Arleo, A., Smeraldi, F., Gerstner, W.: Cognitive navigation based on nonuniform Gabor space sampling, unsupervised growing networks, and reinforcement learning. IEEE Trans. Neural Netw. **15**(3), 639–652 (2004)
5. Barrera, A., Caceres, A., Weitzenfeld, A., Ramirez-Amaya, V.: Comparative experimental studies on spatial memory and learning in rats and robots. J. Intell. Robot. Syst. **63**(3-4), 361–397 (2011)
6. Barrera, A., Tejera, G., Llofriu, M., Weitzenfeld, A.: Learning spatial localization: From rat studies to computational models of the hippocampus. Spat. Cogn. Comput. **15**(1), 27–59 (2015)
7. Barrera, A., Weitzenfeld, A.: Biologically-inspired robot spatial cognition based on rat neurophysiological studies. J. Auto. Robot. Springer **25**(1-2), 147–169 (2008)
8. Barto, A.G.: Adaptive critics and the basal ganglia. In: Houk, C., Davis, J.L., Beiser, D. (Eds.), Models ofinformation processing in the basal ganglia, MIT Press Cambridge MA pp. 215-232 (1995)
9. Borenstein, J., Feng, L.: Measurement and correction of systematic odometry errors in mobile robots. IEEE Trans. Robot. Autom. **12**, 869–880 (1996)
10. Brown, M.A., Sharp, P.E.: Simulation of spatial learning in the morris water maze by a neural network model of the hippocampal formation and nucleus accumbens. Hippocampus **5**, 171–188 (1995)
11. Burak, Y., Fiete, I.R.: Accurate path integration in continuous attractor network models of grid cells, PLoS Comput. Biol (2009)
12. Burgess, N., Recce, M., O'Keefe, J.: A model of hippocampal function. Neural Netw. **7**(6-7), 1065–1081 (1994)
13. Burgess, N., Barry, C., O'Keefe, J.: An Oscillatory Interference Model of Grid Cell Firing. Hippocampus **17**, 801–812 (2007)
14. Bush, D., Burgess, N.: A hybrid oscillatory interference / continuous attractor network model of grid cell firing. J. Neurosci. **34**, 5065–5079 (2014)
15. Caluwaerts, K., Staffa, M., N'Guyen, S., Grand, C., Dollé, L., Favre-Felix, A., Girard, B., Khamassi, M.: A biologically inspired meta-control navigation system for the Psikharpax rat robot. IOP Bioinspiration & Biomimetics **7**(2), 025009 (2012). https://doi.org/10.1088/1748-3182/7/2/025009
16. Cheung, A., Ball, D., Milford, M., Wyeth, G., Wiles, J.: Maintaining a cognitive map in darkness: The need to fuse boundary knowledge with path integration. PLoS Comput. Biol. **8**(8) (2012). https://doi.org/10.1371/journal.pcbi.1002651
17. Cho, J., Sharp, P.: Head direction, place, and movement correlates for cells in the rat retrosplenial cortex. Behav. Neurosci. **115**(1), 3–25 (2001)
18. Dollé, L., Sheynikhovich, D., Girard, B., Chavarriaga, R., Guillot, A.: Path planning versus cue responding: a bioinspired model of switching between navigation strategies. Biol. Cybern. **103**(4), 299–317 (2010)
19. Etienne, A.S., Jeffery, K.J.: Path integration in mammals. Hippocampus **14**(2), 180–192 (2004)
20. Filliat, D., Meyer, J.-A.: Global localization and topological map learning for robot navigation, From Animals to Animats 7, Proceedings of the Seventh International Conference on Simulation of Adaptive Behavior, edited by Hallam et al The MIT Press pp. 131-140 (2002)
21. Fuhs, M.C., Touretzky, D.S.: A spin glass model of path integration in rat medial entorhinal cortex. J. Neurosci. **26**, 4266–4276 (2006)
22. Fyhn, M., Molden, S., Witter, M., Moser, E., Moser, M.B.: Spatial representation in the entorhinal cortex, Science, Vol 305 pp 1258-1264 Sept (2004)
23. Gaussier, P., Revel, A., Banquet, J.P., Babeau, V.: From view cells and place cells to cognitive map learning: processing stages of the hippocampal system. Biol. Cybern. **86**, 15–28 (2002)
24. Gibson, J.J.: The visual perception of objective motion and subjective movement. Psychol. Rev. **61**, 304–314 (1954)

25. Gibson, J.J.: The theory of affordances. In: Shaw, R., Bransford, J. (eds.) Perceiving, acting, and knowing: Toward an ecological psychology, pp. 67–82. Erlbaum, Hillsdale (1977)
26. Granon, S., Poucet, B.: Involvement of the rat prefrontal cortex in cognitive functions: A central role for the prelimbic area. Psychobiology **28**(2), 229–237 (2000)
27. Guazzelli, A., Corbacho, F.J., Bota, M., Arbib, M.A.: Affordances, motivation, and the world graph theory. Adapt. Behav. **6**(3-4), 435–471 (1998)
28. Guzowski, J.F., Knierim, J.J., Moser, E.I.: Ensemble dynamics of hippocampal regions CA3 and CA1. Neuron **44**(4), 581–584 (2004)
29. Hafting, T., Fyhn, M., Molden, S., Moser, M.B., Moser, E.: Microstructure of a spatial map in the entorhinal cortex, Nature, Vol 436 pp 801-806 Aug (2005)
30. Hasselmo, M., Giocomo, M., Zilli, E.: Grid cell firing may arise from interference of theta frequency membrane potential oscillations in single neurons. Hippocampu,s **17**, 1252–1271 (2007)
31. Hebb, D.O.: The organization of behavior: a neuropsychological theory. Wiley-Interscience, New York (1949)
32. Houk, J.C., Adams, J.L., Barto, A.G.: In Models of information processing in the basal ganglia, edited by J. C. Houk, J. L. Davis and D. G. Beiser, MIT Press, pp. 249–270 (1995)
33. Jeffery, K.J., O'Keefe, J.M.: Learned interaction of visual and idiothetic cues in the control of place field orientation. Exp. Brain Res. **127**, 151–161 (1999)
34. Kelley, A.: Ventral striatal control of appetitive motivation: role in ingestive behavior and reward-related learning. Neurosci. Biobehav. Rev. **27**(8), 765–776 (2004)
35. Krupic, J., Burgess, N., O'Keefe, J.: Neural representations of location composed of spatially periodic bands. Science **337**, 853–857 (2012)
36. Leutgeb, S., Leutgeb, J.K., Treves, A., Moser, M.B., Moser, E.: Distinct ensemble codes in hippocampal areas CA3 and CA1. Science **305**(5688), 1295–1298 (2004)
37. Leutgeb, S., Leutgeb, J.K.: Pattern separation, pattern completion, and new neuronal codes within a continuous CA3 map. Learn. Mem. **14**(11), 745–57 (2007)
38. McNaughton, B., Battaglia, F., Jensen, O., Moser, E., Moser, M.B.: Path integration and the neural basis of the 'cognitive map', Nature Reviews Neuroscience, Vol 7 pp 663-678 Aug (2006)
39. McNaughton, B., Knierim, J.J., Wilson, M.A.: Vector encoding and the vestibular foundations of spatial cognition. In: Gazzaniga, M. (Ed), The cognitive neurosciences. MIT Press Boston, pp. 585–595 (1994)
40. McNaughton, B., Mizumori, S., Barnes, C., Leonard, B., Marquis, M., Green, E.: Cortical representation of motion during unrestrained spatial navigation in the rat. Cereb. Cortex **4**, 27–39 (1994)
41. Mhatre, H., Gorchetchnikov, A., Grossberg, S.: Grid cell hexagonal patterns formed by fast self-organized learning within entorhinal cortex. Hippocampus **22**(2), 320–334 (2012)
42. Milford, M., Wyeth, G.: Spatial mapping and map exploitation: a bio-inspired engineering perspective. In: Winter, S., Duckham, M., Kulik, L., Kuipers, B. (eds.) Spatial Information Theory, pp. 203–221. Springer-Verlag, Heidelberg (2007)
43. Milford, M., Wyeth, G.: Persistent navigation and mapping using a biologically inspired SLAM system. Int. J. Robot. Res. **29**(9), 1131–1153 (2010)
44. Mittelstaedt, M., Mittelstaedt, H.: Homing by path integration in a mammal. In: Papi, F., Wallraff, H.G. (eds.) Avian Navigation, pp. 290–297. Springer Verlag, Berlin (1982)
45. Morris, R.G.M.: Spatial localization does not require the presence of local cues, Learning and Motivation, vol. 12, pp. 239 –260 (1981)
46. Morris, R.G.M.: Developments of a water-maze procedure for studying spatial learning in the rat. J. Neurosci. Methods **11**, 47–60 (1984). Elsevier
47. Moser, E., Kropff, E., Moser, M.B.: Place cells, grid cells, and the brain's spatial representation system. Annu. Rev. Neurosci. **31**, 69–89 (2008)
48. Navratilova, Z., Giocomo, L.M., Fellous, J.M., Hasselmo, M., McNaughton, B.: Phase precession and variable spatial scaling in a periodic attractor map model of medial Entorhinal grid cells with realistic after-spike dynamics, Hippocampus (2011)
49. O'Keefe, J., Conway, D.H.: Hippocampal place units in the freely moving rat: why they fire where they fire. Exp. Brain Res. **31**, 573–590 (1978)
50. O'Keefe, J., Nadel, L.: The hippocampus as a cognitive map. Oxford University Press, Oxford (1978)
51. O'Keefe, J., Dostrovsky, J.: The hippocampus as a spatial map: preliminary evidence from unit activity in the freely moving rat. Brain Res. **34**(1), 171–175 (1971)
52. O'Keefe, J.: Spatial memory within and without the hippocampal system, in Neurobiology of the Hippocampus. In: Seifert, W. (ed.), pp. 375–403. Academic Press, New York (1983)
53. Parron, C., Save, E.: Evidence for entorhinal and parietal cortices involvement in path integration in the rat. Exp. Brain Res. **159**(3), 349–359 (2004)
54. Poucet, B.: Spatial cognitive maps in animals: new hypotheses on their structure and neural mechanisms. Psychol. Rev. **100**(2), 163–182 (1993)
55. Quirk, G.J., Muller, R.U., Kubie, J.L.: The firing of hippocampal place cells in the dark depends on the rat's recent experience. J. Neurosci. **10**(6), 2008–2017 (1990)
56. Ranck, J.B.J.r.: Head-direction cells in the deep layers of dorsal presubiculum in freely moving rats. Soc. Neurosci. Abstr. **10**, 599 (1984)
57. Redish, A., Touretzky, D.: Cognitive maps beyond the hippocampus. Hippocampus **7**(1), 15–35 (1997)
58. Rolls, E.T.: Head direction and spatial view cells in primates, and brain mechanisms for path integration. In: Head direction cells and the neural mechanisms underlying directional orientation, pp. 299–318. MIT Press, Cambridge (2005)
59. Samu, D., Erős, P., Ujfalussy, B., Kiss, T.: Robust path integration in the entorhinal grid cell system with hippocampal feed-back. Biol. Cybern. **101**(1), 19–34 (2009)
60. Schultz, W., Tremblay, L., Hollerman, J.: Reward prediction in primate basal ganglia and frontal cortex. Neuropharmacology **37**(4-5), 421–429 (1998)
61. Solstad, T., Moser, E.I., Einevoll, G.T.: From grid cells to place cells: a mathematical model. Hippocampus **16**, 1026–1031 (2006)
62. Taube, J.S., Muller, R.I., Ranck, J.B.J.r.: Head direction cells recorded from the postsubiculum in freely moving rats. II. Effects of environmental manipulations. J. Neurosci. **10**, 436–447 (1990)
63. Taube, J.S.: Head direction cells and the neurophysiological basis for a sense of direction. Prog. Neurobiol. **55**, 225–56 (1998)
64. Tejera, G., Barrera, A., Llofriu, M., Weitzenfeld, A.: Solving uncertainty during robot navigation by integrating grid cell and place cell firing based on rat spatial cognition studies, International Conference on Advanced Robotics, Proc. ICAR 2013, Montevideo, Uruguay (2013)
65. Tejera, G., Llofriu, M., Barrera, A., Weitzenfeld, A.: A Spatial Cognition Model Integrating Grid Cells and Place Cells. In: International Joint Conference on Neural Networks, Proc. IJCNN 2015, July 12-17, Killarney, Ireland (2015)
66. Tolman, E.: Cognitive maps in rats and men. Psychol. Rev. **55**, 189–208 (1948)

67. Towse, B., Barry, C., Bush, D., Burgess, N.: Optimal configurations of spatial scale for grid cell firing under noise and uncertainty, Philosophical Transaction of the Royal Society (2013)
68. Weitzenfeld, A., Arbib, M., Alexander A. MIT Press, Cambridge (2002)

Gonzalo Tejera is a Professor in the Institute of Computing at the Department of Ingeniería at the Universidad de la República (UDELAR) in Montevideo, Uruguay, where he obtained his BS, MS and PhD. His research line is focused in Bio-inspired Navigation: understanding the mechanisms underlying the process of spatial cognition in rodents in order to relate the physiological data concerning such process in a robotic architecture.

Martin Llofriu obtained his MS and PhD in the Department of Computer Science and Engineering at the College of Engineering in the University of South Florida in Tampa, Florida, USA. Prior to that, Dr. Llofriu obtained a BS, in computer Engineering from Department of Ingeniería at the Universidad de la República (UDELAR) in Montevideo, Uruguay. His research interests are in robotics.

Alejandra Barrera is a Full-time Professor in the Engineering Division of the Autonomous Technological Institute of Mexico (ITAM). She obtained the degree of Computer Engineering and master's degree in Information Technology and Management at ITAM, and a doctorate degree in Engineering from the National Autonomous University of Mexico (UNAM). She has received recognition for academic excellence from the Mexican Association of Mechanical and Electrical Engineers (AMIME), the National Association of Faculties and Engineering Schools (ANFEI), and ITAM (Palacios Macedo Medal). Her research interests include Biorobotics, Data Analysis, Data Visualization and Business Intelligence. She is the author of several research articles and editor of some international books. Since 2013, she is part of the Editorial Committee of the International Journal of Advanced Robotic Systems.

Alfredo Weitzenfeld is a Professor in the Department of Computer Science and Engineering at the College of Engineering in the University of South Florida in Tampa, Florida, USA. Dr. Weitzenfeld received a PhD in Computer Science and an MS in Computer Engineering from the University of Southern California in Los Angeles, California, USA. He received a BS in Electrical Engineering from the Technion in Haifa, Israel. Dr. Weitzenfeld is the Director of the Biorobotics Laboratory and the USF RoboBulls robot soccer teams at USF. His main research interests are in the areas of biologically inspired robotics, neurobotics, neural computational modeling, humanoid robots, cognitive, and multi-robot systems. Dr. Weitzenfeld has authored 2 books and over 130 refereed journal and conference papers.